Supporting Information

$(C_{13}N_3H_{14})_2MBr_4$ (M=Zn, Cd): Two Novel Hybrid Metal Halides with Balanced Integrated Nonlinear Optical Performance

Jiajing Wu*, Yi-Fan Fu, Wenlong Liu, and Sheng-Ping Guo*

School of Chemistry and Chemical Engineering, Yangzhou University, Yangzhou, Jiangsu 225002, P. R. China.

E-mail: jiajingw@yzu.edu.cn, spguo@yzu.edu.cn.

Contents

Figure S1. (a) The structure of **2** along the *c*-axis; (b) The inorganic and organic parts rotating along the *c* axis with 2_1 helical symmetry; (c) The organic layers in the *ac* plane; (d) The inorganic layers in the *bc* plane and their dipole moments. Hydrogen atoms are omitted for clarity.

Figure S2. Hydrogen bonds in **1** (a) and **2** (b).

Figure S3. Dipole moments of $[MBr_4]^{2-}$ and $C_{13}N_3H_{14}^+$ in one-unit cell. (a) **1**; (b) **2**. Blue: $[MBr_4]^{2-}$; orange and purple: $C_{13}N_3H_{14}^+$. The red arrows in the middle present the total dipole moments of the inorganic parts and organic parts, respectively.

Figure S4. Simulated and experimental powder X-ray diffraction patterns of **1** and **2**.

Figure S5. The TGA curves of **1** (a) and **2** (b).

Figure S6. Crystal photographs of **1** (a) and **2** (b).

Figure S7 Distribution of C and Zn/Cd atoms in unit cells of **1** (a) and **2** (b).

Figure S8. Calculated frequency-dependent NLO coefficients of **1** (a) and **2** (b).

Table S1. Crystal data and structural refinement for **1** and **2**.

Empirical formula	$(C_{13}N_3H_{14})_2ZnBr_4$ (**1**)	$(C_{13}N_3H_{14})_2CdBr_4$ (**2**)
Formula weight/g mol^{-1}	809.55	856.58
Temperature/K	296	296
Crystal system	orthorhombic	orthorhombic
Space group	$Pna2_1$	$Pna2_1$
a/Å	12.9297(7)	13.0023(5)
b/Å	14.7057(7)	14.6412(5)
c/Å	15.9445(7)	16.1558(6)
α/°	90	90
β/°	90	90
γ/°	90	90
Volume/Å^3	3031.7(3)	3075.6(2)
Z	4	4
ρ_{calC}(g/cm^3)	1.774	1.85
μ/mm^{-1}	6.108	5.932
F(000)	1584.0	1656.0
2θ range (deg)	4.912 - 55.122	4.19 - 55.162
Index ranges	$-16 \leq h \leq 16$, $-15 \leq k \leq 19$, $-20 \leq l \leq 20$	$-16 \leq h \leq 16$, $-19 \leq k \leq 18$, $-21 \leq l \leq 20$
Reflections collected	45996	46484
Independent reflections	6959 [R_{int} = 0.0579, R_{sigma} = 0.0495]	7086 [R_{int}= 0.0826, R_{sigma}= 0.0791]

Table S1. Crystal data and structural refinement for **1** and **2**.

GOF on F^2	1.021	1.004
Final R indexes [I ≥ 2σ (I)]	R1 = 0.0352, wR2 = 0.0564	R1 = 0.0420, wR2 = 0.0430
Final R indexes [all data]	R1 = 0.0620, wR2 = 0.0625	R1 = 0.0920, wR2 = 0.0498
Δρ_{max}, Δρ_{min} /e Å^{-3}	0.34/-0.56	0.40/-0.50
Flack parameter	0.011 (5)	0.000(5)

R1 = $\Sigma||Fo|-|Fc|| / \Sigma|Fo|$, wR2 = $\{\Sigma[w(|Fo|^2 - |Fc|^2)^2] / \Sigma[w(|Fo|^4)]\}^{1/2}$ and w = $1/[\sigma^2(Fo^2)+(0.0462P)^2]$，

where P = $(Fo^2+2Fc^2)/3$.

Table S2. Fractional atomic coordinates ($\times 10^4$) and equivalent isotropic displacement parameters (Å^2 $\times 10^3$) for **1** and **2**. U_{eq} is defined as 1/3 of the trace of the orthogonalized U_{ij} tensor.

Atom	x	y	z	U_{eq}
		(1)		
Br(1)	3690.4(4)	7058.1(3)	6658.0(4)	38.06(13)
Br(2)	2880.8(5)	5854.3(4)	4638.8(3)	40.41(15)
Br(3)	1032.8(4)	5894.5(4)	6632.3(5)	51.19(17)
Zn(1)	2774.1(5)	5689.7(4)	6147.5(4)	36.10(16)
Br(4)	3537.6(5)	4317.4(4)	6616.7(5)	54.31(17)
N(2)	6885(4)	6542(3)	5762(3)	46.0(12)
N(5)	4146(4)	2706(3)	2947(3)	48.7(13)
N(4)	3937(3)	3822(3)	3944(3)	43.2(12)
N(6)	2519(3)	3093(3)	3363(3)	40.2(12)
N(3)	5492(4)	5999(3)	5013(3)	46.4(13)
C(7)	3537(4)	3210(4)	3423(3)	34.4(13)
C(20)	6123(4)	6661(4)	5208(3)	38.3(14)
N(1)	6016(5)	7457(4)	4845(4)	68.7(17)
C(5)	5374(3)	3623(3)	4895(2)	44.6(14)
C(4)	6420(3)	3704(3)	5084(2)	59.3(18)
C(3)	7096(2)	4076(3)	4500(3)	63(2)
C(2)	6727(3)	4366(3)	3726(3)	63(2)

Table S2. Fractional atomic coordinates ($\times 10^4$) and equivalent isotropic displacement parameters ($\text{Å}^2 \times 10^3$) for **1** and **2**. U_{eq} is defined as 1/3 of the trace of the orthogonalized U_{ij} tensor.

Atom	x	y	z	U_{eq}
C(1)	5682(3)	4285(3)	3536.8(19)	48.3(16)
C(6)	5005(2)	3914(3)	4121(2)	35.5(13)
C(18)	6278(2)	5353(3)	6713(3)	48.4(14)
C(17)	6488(3)	4606(3)	7220(3)	56.7(17)
C(16)	7490(4)	4270(3)	7274(3)	60.6(19)
C(15)	8283(2)	4680(3)	6822(3)	57.5(17)
C(14)	8072(2)	5427(3)	6316(2)	48.0(16)
C(19)	7070(3)	5763(2)	6261(2)	40.6(14)
C(10)	188(3)	4263(3)	4838(3)	77(2)
C(11)	1035(3)	3863(3)	5228.6(17)	61.9(19)
C(12)	1819(3)	3479(2)	4749(2)	43.6(14)
C(13)	1757(3)	3495(2)	3879(2)	36.6(13)
C(8)	910(3)	3895(3)	3488.3(18)	52.4(16)
C(9)	126(3)	4279(3)	3968(3)	79(2)
C(22)	4438(4)	8189(3)	4390(3)	79(2)
C(21)	5308(3)	7673(3)	4199(3)	50.3(16)
C(26)	5490(3)	7404(3)	3376(3)	73(2)
C(25)	4803(5)	7650(4)	2746(2)	91(3)

Table S2. Fractional atomic coordinates ($\times 10^4$) and equivalent isotropic displacement parameters (Å^2 $\times 10^3$) for **1** and **2**. U_{eq} is defined as 1/3 of the trace of the orthogonalized U_{ij} tensor.

Atom	x	y	z	U_{eq}
C(24)	3934(4)	8166(4)	2937(4)	85(3)
C(23)	3751(3)	8436(3)	3760(4)	101(3)
		(2)		
Cd(1)	2757.6(3)	4416.0(3)	6088.7(3)	39.87(13)
Br(2)	2919.6(5)	4135.9(4)	4509.5(4)	41.35(18)
Br(1)	3674.4(5)	2916.3(4)	6644.3(5)	40.15(16)
Br(3)	921.3(5)	4161.6(5)	6632.0(5)	54.5(2)
Br(4)	3574.3(6)	5894.8(5)	6580.1(6)	59.7(2)
N(3)	3972(4)	6150(3)	3848(3)	40.9(15)
N(1)	4178(4)	7306(4)	2903(4)	51.4(17)
N(2)	2563(4)	6906(4)	3310(3)	39.8(15)
N(6)	6861(4)	3474(4)	5755(3)	48.7(16)
C(7)	3573(5)	6780(4)	3355(4)	34.7(17)
N(5)	5495(4)	3987(3)	4989(3)	47.3(16)
C(8)	5046(5)	6050(4)	4026(4)	39.3(18)
C(6)	1859(5)	6547(4)	4677(4)	41.4(18)
C(9)	5694(5)	5650(5)	3464(4)	53(2)
C(5)	1099(6)	6160(5)	5145(5)	58(2)

Table S2. Fractional atomic coordinates ($\times 10^4$) and equivalent isotropic displacement parameters ($\text{Å}^2 \times 10^3$) for **1** and **2**. U_{eq} is defined as 1/3 of the trace of the orthogonalized U_{ij} tensor.

Atom	x	y	z	U_{eq}
C(20)	6108(5)	3334(5)	5207(4)	38.2(17)
C(13)	5414(6)	6357(5)	4770(4)	46.2(19)
C(10)	6722(6)	5554(6)	3643(5)	67(3)
C(21)	7036(5)	4278(4)	6231(4)	39.4(18)
C(14)	5296(7)	2285(4)	4221(5)	50(2)
C(25)	6480(7)	5461(5)	7128(5)	58(2)
C(1)	1808(5)	6496(4)	3827(4)	33.9(17)
C(12)	6448(7)	6251(5)	4940(5)	57(2)
C(11)	7104(6)	5862(6)	4377(6)	62(2)
C(17)	3955(8)	1781(6)	3009(7)	76(3)
C(22)	8029(5)	4619(5)	6269(4)	50(2)
C(18)	4823(8)	2256(6)	2818(5)	88(3)
C(26)	6266(5)	4703(5)	6670(5)	47.2(17)
C(23)	8225(6)	5368(5)	6745(5)	60(2)
N(4)	5998(5)	2526(4)	4855(4)	75(2)
C(2)	988(6)	6076(5)	3456(5)	54(2)
C(19)	5493(6)	2501(5)	3419(6)	69(2)
C(24)	7439(7)	5805(5)	7173(5)	61(2)

Table S2. Fractional atomic coordinates ($\times 10^4$) and equivalent isotropic displacement parameters ($\text{Å}^2 \times 10^3$) for **1** and **2**. U_{eq} is defined as 1/3 of the trace of the orthogonalized U_{ij} tensor.

Atom	x	y	z	U_{eq}
C(4)	277(6)	5729(6)	4770(6)	77(3)
C(3)	220(6)	5690(6)	3920(6)	82(3)
C(15)	4422(8)	1826(5)	4426(6)	72(2)
C(16)	3748(8)	1570(6)	3814(8)	86(3)

Table S3. Bond lengths for **1** and **2**.

Atom	Atom	Length/Å	Atom	Atom	Length/Å
		(1)			
Br(1)	Zn(1)	2.4729(8)	C(1)	C(6)	1.39
Br(2)	Zn(1)	2.4217(9)	C(18)	C(17)	1.39
Br(3)	Zn(1)	2.3995(8)	C(18)	C(19)	1.39
Zn(1)	Br(4)	2.3680(8)	C(17)	C(16)	1.39
N(2)	C(20)	1.334(7)	C(16)	C(15)	1.39
N(2)	C(19)	1.416(5)	C(15)	C(14)	1.39
N(5)	C(7)	1.320(7)	C(14)	C(19)	1.39
N(4)	C(7)	1.330(7)	C(10)	C(11)	1.39
N(4)	C(6)	1.417(5)	C(10)	C(9)	1.39
N(6)	C(7)	1.331(6)	C(11)	C(12)	1.39
N(6)	C(13)	1.414(5)	C(12)	C(13)	1.39
N(3)	C(20)	1.307(7)	C(13)	C(8)	1.39
C(20)	N(1)	1.314(7)	C(8)	C(9)	1.39
N(1)	C(21)	1.414(6)	C(22)	C(21)	1.39
C(5)	C(4)	1.39	C(22)	C(23)	1.39
C(5)	C(6)	1.39	C(21)	C(26)	1.39
C(4)	C(3)	1.39	C(26)	C(25)	1.39
C(3)	C(2)	1.39	C(25)	C(24)	1.39

Table S3. Bond lengths for **1** and **2**.

Atom	Atom	Length/Å	Atom	Atom	Length/Å
C(2)	C(1)	1.39	C(24)	C(23)	1.39

(2)

Atom	Atom	Length/Å	Atom	Atom	Length/Å
Cd(1)	Br(2)	2.5926(9)	C(13)	C(12)	1.381(9)
Cd(1)	Br(1)	2.6549(8)	C(10)	C(11)	1.362(11)
Cd(1)	Br(3)	2.5710(8)	C(21)	C(22)	1.385(8)
Cd(1)	Br(4)	2.5388(8)	C(21)	C(26)	1.375(8)
N(3)	C(7)	1.325(8)	C(14)	N(4)	1.417(9)
N(3)	C(8)	1.433(8)	C(14)	C(19)	1.358(10)
N(1)	C(7)	1.321(7)	C(14)	C(15)	1.361(11)
N(2)	C(7)	1.329(7)	C(25)	C(26)	1.363(9)
N(2)	C(1)	1.421(7)	C(25)	C(24)	1.346(11)
N(6)	C(20)	1.335(8)	C(1)	C(2)	1.369(9)
N(6)	C(21)	1.425(8)	C(12)	C(11)	1.371(10)
N(5)	C(20)	1.294(7)	C(17)	C(18)	1.361(11)
C(8)	C(9)	1.370(9)	C(17)	C(16)	1.364(12)
C(8)	C(13)	1.369(9)	C(22)	C(23)	1.364(9)
C(6)	C(5)	1.367(9)	C(18)	C(19)	1.354(11)
C(6)	C(1)	1.377(9)	C(23)	C(24)	1.389(10)
C(9)	C(10)	1.374(10)	C(2)	C(3)	1.370(10)

Table S3. Bond lengths for **1** and **2**.

Atom	Atom	Length/Å	Atom	Atom	Length/Å
C(5)	C(4)	1.381(10)	C(4)	C(3)	1.376(12)
C(20)	N(4)	1.320(8)	C(15)	C(16)	1.374(12)

Table S4. Bond angles for **1** and **2**.

Atom	Atom	Atom	Angle/°	Atom	Atom	Atom	Angle/°
			(1)				
Br(2)	Zn(1)	Br(1)	102.61(3)	C(17)	C(18)	C(19)	120
Br(3)	Zn(1)	Br(1)	103.97(3)	C(16)	C(17)	C(18)	120
Br(3)	Zn(1)	Br(2)	111.16(4)	C(15)	C(16)	C(17)	120
Br(4)	Zn(1)	Br(1)	112.94(3)	C(16)	C(15)	C(14)	120
Br(4)	Zn(1)	Br(2)	112.04(3)	C(15)	C(14)	C(19)	120
Br(4)	Zn(1)	Br(3)	113.35(4)	C(18)	C(19)	N(2)	121.2(3)
C(20)	N(2)	C(19)	127.1(4)	C(14)	C(19)	N(2)	118.7(3)
C(7)	N(4)	C(6)	124.6(4)	C(14)	C(19)	C(18)	120
C(7)	N(6)	C(13)	126.5(4)	C(11)	C(10)	C(9)	120
N(5)	C(7)	N(4)	120.5(5)	C(12)	C(11)	C(10)	120
N(5)	C(7)	N(6)	118.4(5)	C(11)	C(12)	C(13)	120
N(4)	C(7)	N(6)	121.1(5)	C(12)	C(13)	N(6)	122.2(3)
N(3)	C(20)	N(2)	121.4(5)	C(12)	C(13)	C(8)	120
N(3)	C(20)	N(1)	119.5(5)	C(8)	C(13)	N(6)	117.8(3)
N(1)	C(20)	N(2)	119.1(5)	C(9)	C(8)	C(13)	120
C(20)	N(1)	C(21)	126.1(5)	C(8)	C(9)	C(10)	120
C(4)	C(5)	C(6)	120	C(21)	C(22)	C(23)	120
C(5)	C(4)	C(3)	120	C(22)	C(21)	N(1)	119.1(4)

Table S4. Bond angles for **1** and **2**.

Atom	Atom	Atom	Angle/°	Atom	Atom	Atom	Angle/°
C(2)	C(3)	C(4)	120	C(26)	C(21)	N(1)	120.9(4)
C(3)	C(2)	C(1)	120	C(26)	C(21)	C(22)	120
C(2)	C(1)	C(6)	120	C(21)	C(26)	C(25)	120
C(5)	C(6)	N(4)	118.8(3)	C(24)	C(25)	C(26)	120
C(1)	C(6)	N(4)	121.2(3)	C(25)	C(24)	C(23)	120
C(1)	C(6)	C(5)	120	C(24)	C(23)	C(22)	120

(2)

Atom	Atom	Atom	Angle/°	Atom	Atom	Atom	Angle/°
Br(2)	Cd(1)	Br(1)	99.52(3)	C(26)	C(21)	N(6)	122.4(6)
Br(3)	Cd(1)	Br(2)	112.86(3)	C(26)	C(21)	C(22)	119.5(7)
Br(3)	Cd(1)	Br(1)	100.47(3)	C(19)	C(14)	N(4)	120.7(8)
Br(4)	Cd(1)	Br(2)	114.12(3)	C(19)	C(14)	C(15)	120.3(8)
Br(4)	Cd(1)	Br(1)	114.32(3)	C(15)	C(14)	N(4)	119.0(8)
Br(4)	Cd(1)	Br(3)	113.90(3)	C(24)	C(25)	C(26)	121.5(8)
C(7)	N(3)	C(8)	125.0(5)	C(6)	C(1)	N(2)	122.0(6)
C(7)	N(2)	C(1)	126.3(5)	C(2)	C(1)	N(2)	118.1(7)
C(20)	N(6)	C(21)	127.0(6)	C(2)	C(1)	C(6)	119.9(6)
N(3)	C(7)	N(2)	121.1(6)	C(11)	C(12)	C(13)	121.4(7)
N(1)	C(7)	N(3)	120.3(6)	C(10)	C(11)	C(12)	119.2(8)
N(1)	C(7)	N(2)	118.6(6)	C(18)	C(17)	C(16)	119.7(9)

Table S4. Bond angles for **1** and **2**.

Atom	Atom	Atom	Angle/°	Atom	Atom	Atom	Angle/°
C(9)	C(8)	N(3)	120.7(7)	C(23)	C(22)	C(21)	119.3(7)
C(13)	C(8)	N(3)	118.9(7)	C(19)	C(1)	C(17)	120.4(9)
C(13)	C(8)	C(9)	120.5(7)	C(25)	C(26)	C(21)	119.9(7)
C(5)	C(6)	C(1)	119.7(7)	C(22)	C(23)	C(24)	120.8(7)
C(8)	C(9)	C(10)	120.1(7)	C(20)	N(4)	C(14)	127.2(6)
C(6)	C(5)	C(4)	120.4(7)	C(1)	C(2)	C(3)	120.8(8)
N(5)	C(20)	N(6)	121.3(6)	C(18)	C(19)	C(14)	120.1(8)
N(5)	C(20)	N(4)	118.5(6)	C(25)	C(24)	C(23)	118.9(8)
N(4)	C(20)	N(6)	120.2(6)	C(3)	C(4)	C(5)	119.9(8)
C(8)	C(13)	C(12)	118.5(7)	C(2)	C(3)	C(4)	119.3(8)
C(11)	C(10)	C(9)	120.3(8)	C(14)	C(15)	C(16)	119.5(9)
C(22)	C(21)	N(6)	118.0(6)	C(17)	C(16)	C(15)	119.9(9)

Table S5. Hydrogen bond lengths (Å) for **1** and **2**.

D–H	d(D–H)	d(H…A)	d(D…A)	∠(D–H…A)(°)	A
			(1)		
N(1)–H(1)	0.86	2.72	3.477(6)	148	Br(2)[#1]
N(2)–H(2)	0.86	2.63	3.425(5)	153	Br(1)[#1]
N(3)–H(3A)	0.86	2.78	3.435(5)	135	Br(2)
N(4)–H(4)	0.86	2.68	3.468(4)	152	Br(2)
N(5)–H(5A)	0.86	2.87	3.489(5)	130	Br(1)[#2]
N(5)–H(5B)	0.86	2.61	3.398(5)	154	Br(3)[#3]
N(6)–H(6)	0.86	2.65	3.486(5)	163	Br(1)[#3]
			(2)		
N(1)–H(1A)	0.86	2.85	3.470(6)	131	Br(1)[#4]
N(1)–H(1B)	0.86	2.63	3.408(6)	152	Br(3)[#5]
N(2)–H(2)	0.86	2.64	3.467(5)	161	Br(1)[#5]
N(3)–H(3)	0.86	2.63	3.422(5)	154	Br(2)
N(4)–H(4A)	0.86	2.81	3.532(6)	142	Br(2)[#6]
N(5)–H(5A)	0.86	2.77	3.444(5)	136	Br(2)
N(6)–H(6A)	0.86	2.63	3.430(5)	155	Br(1)[#6]

Symmetry transformations used to generate equivalent atoms: #1 1/2+*x*, 3/2-*y*, *z*; #2 1-*x*, 1-*y*, -1/2+*z*; #3 1/2-*x*, -1/2+*y*, -1/2+*z*; #4 1-*x*, 1-*y*, -1/2+*z*; #5 1/2-*x*, 1/2+*y*, -1/2+*z*; #6 1/2+*x*, 1/2-*y*, *z*.

Table S6. The *x*/*y*/*z*-projections of local dipole moments (DM) of $[ZnBr_4]^{2-}$ and $[CdBr_4]^{2-}$ in one-unit cell of **1** and **2**.

Ion	μ_x (D)	μ_y (D)	μ_z (D)
(1)			
$[ZnBr_4]^{2-}$	-0.382523	-2.7583769	0.35409998
$[ZnBr_4]^{2-}$	0.38043	2.75777824	0.35409998
$[ZnBr_4]^{2-}$	0.38093562	-2.7548558	0.355347
$[ZnBr_4]^{2-}$	-0.3820174	2.75780178	0.355347
Total $[ZnBr_4]^{2-}$	-0.003174815	0.002347358	1.418893948
(2)			
$[CdBr_4]^{2-}$	-0.451625215	3.260348857	0.006384011
$[CdBr_4]^{2-}$	0.451625215	-3.260348857	0.006384011
$[CdBr_4]^{2-}$	0.451625215	3.260348857	0.006384011
$[CdBr_4]^{2-}$	-0.451625215	-3.260348857	0.006384011
Total $[CdBr_4]^{2-}$	-1.73195E-14	1.59872E-14	0.025536044

Table S7. The bond distortion degree (Δd) and bond angle distortion (σ^2) of the ZnBr$_4$ (**1**) and CdBr$_4$ (**2**) tetrahedra.

Compound	bond	distance/Å	d_0/Å	Δd
1	Zn(1)–Br(1)	2.4729	2.4155	2.52×10^{-4}
	Zn(1)–Br(2)	2.4217		
	Zn(1)–Br(3)	2.3995		
	Zn(1)–Br(4)	2.3680		
2	Cd(1)–Br(1)	2.6549	2.5895	2.68×10^{-4}
	Cd(1)–Br(2)	2.5926		
	Cd(1)–Br(3)	2.5710		
	Cd(1)–Br(4)	2.5388		

Compound	Angle	Angle/°	θ_0/°	σ^2
1	Br(2)–Zn(1)–Br(1)	102.61	109.5	22.7824
	Br(3)–Zn(1)–Br(1)	103.97		
	Br(3)–Zn(1)–Br(2)	111.16		
	Br(4)–Zn(1)–Br(1)	112.94		
	Br(4)–Zn(1)–Br(2)	112.04		
	Br(4)–Zn(1)–Br(3)	113.35		
2	Br(2)–Cd(1)–Br(1)	99.52	109.5	51.2735
	Br(3)–Cd(1)–Br(1)	100.47		
	Br(3)–Cd(1)–Br(2)	112.86		
	Br(4)–Cd(1)–Br(1)	114.32		
	Br(4)–Cd(1)–Br(2)	114.12		
	Br(4)–Cd(1)–Br(3)	113.90		

Table S8. Linear and nonlinear optical properties of organic-inorganic hybrid ionic metal halides containing d^{10} transition metal cations

Compounds	Space group	SHG efficiency	Band gap (eV)	Birefringence (@1064 nm)	PM	LIDT	Ref
$[N(CH_3)_4]_2HgBr_2I_2$	$P2_12_12_1$	0.46 × KDP	2.8	0.031	√	-	1
$[N(CH_3)_4]_2HgI_4$	$P2_12_12_1$	0.5 × KDP	2.73	0.002	×	-	1
$(TpyH_3)[CdCl_4][Cl]$	$P2_12_12_1$	0.72 × KDP	2.85,	-	×	-	2
$(C_{20}H_{20}P)CuBr_2$	$P2_1$	1.1 × KDP	3.56	0.12	√	-	3
$(C_{20}H_{20}P)CuCl_2$	$P2_1$	0.89 × KDP	3.64	0.13	√	-	3
$NH_4HgBr_3·H_2O$	$Cmm2$	28 × KDP	3.40	0.183	√	52.7 × AGS	4
$[(CH_2)_3NH_2S]CdBr_3$	$Cmc2_1$	0.73 × KDP	-	-	-	-	5
$(C_6H_{14}N)_2CdCl_4$	$Cmc2_1$	0. 6× KDP	-	-	-	-	6
$(C_3N_6H_7)(C_3N_6H_6)HgCl_3$	$P2_1$	5 × KDP	4.4	0.246	√	-	7
$(H_6C_2N)_2CdI_4$	$P2_12_12_1$	0.5 × KDP	3.86	0.047	×	-	8
$\alpha\text{-}(CN_3H_6)_3Cu_2I_5$	$Fdd2$	1.8 × KDP	2.80	-	×	-	9
$(H_7C_3N_6)(H_6C_3N_6)ZnCl_3$	$P2_1$	2.8 × KDP	5.25	0.255	√	-	10
$(S\text{-}PCA)\ CuBr_2$	$C2$	0.3 × KDP	2.7	-	-	-	11
$(S\text{-}PCA)CuBr_2·\ 0.5H_2O$	$C2$	0.4 × KDP	2.87	-	-	-	11
$(S\text{-}PCA)\ CuI_2$	$C2$	0.6 × KDP	3.66	-	-	-	11
$N(CH_3)_4ZnCl_3$	$Pmc2_1$	15 × SiO_2	3.4	-	×	-	12
$([Et_3P(CH_2)_2Cl][Cd(dca)_3]$	$P2_12_12_1$	0.16 × KDP	-	-	-	-	13
$[N(CH_3)_4]\ HgBrI_2$	$Pmc2_1$	4.5 × KDP	2.83	0.025	×	-	14
$[R\text{-}MPA]_2CdCl_4$	Cc	0.53 × KDP	4.418	-	-	-	15
$[Et_3(n\text{-}Pr)P][Cd(dca)_3]$	$P2_12_12_1$	0.12 × KDP	-	-	-	-	16
$(l\text{-}Hpro)_2Cd_5Cl_{12}\ (1L)$	$P1$	0.25 × KDP	4.80	0.05	√	-	17
$(l\text{-}Hpro)(l\text{-}pro)CdCl_3\ (2L)$	$P2_1$	0.7 × KDP	5.10	0.06	√	-	17
$[Me_3NCH_2Cl]CdCl_3$	Cc	0.73 × KDP	5.24	0.043	√	-	18
$(C_{13}N_3H_{14})_2ZnBr_4$	$Pna2_1$	1.22 × KDP	3.96	0.15	√	28 × AGS	This work
$(C_{13}N_3H_{14})_2CdBr_4$	$Pna2_1$	1.14 × KDP	3.98	0.12	√	25 × AGS	This work

Table S9. Point charge model analysis of **1** and **2**. According to the crystal structure data collected at 296 K, we select a unit cell and assume that the centers of the positive charges of the organic cations and the negative charges of the $(ZnBr_4)^{2-}$ and $(CdBr_4)^{2-}$ are located on the C and Cd/Zn atoms, respectively.

(1)		
Atom	Atom coordinate	Coordinate of charge center
Zn(1)	(0.77741, 0.93103, 0.61475)	(0.5, 0.5, 0.36475)
Zn(1)	(0.27741, 0.56897, 0.61475)	
Zn(1)	(0.72259, 0.43103, 0.11475)	
Zn(1')	(0.22259, 0.06897, 0.11475)	
C(7)	(0.8537, 0.179, 0.3423)	(0.5, 0.5, 0.43155)
C(7)	(0.3537, 0.321, 0.3423)	
C(7)	(0.6463, 0.679, 0.8423)	
C(7)	(0.1463, 0.821, 0.8423)	
C(20)	(0.1123, 0.8339, 0.5208)	
C(20)	(0.8877, 0.1661, 0.0208)	
C(20)	(0.3877, 0.3339, 0.0208)	
C(20)	(0.6123, 0.6661, 0.5208)	
$(0.43155 - 0.36475) \times c \times Z \times e = 0.0668 \times 15.9445 \times 10^{-10}$ m $\times 4 \times 1.6 \times 10^{-19}$ C $= 6.8166 \times 10^{-29}$ C·m $= 20.4735$ D		
(2)		
Atom	Atom coordinate	Coordinate of charge center
Cd(1)	(0.27576, 0.4416, 0.60887)	(0.5, 0.5, 0.35887)
Cd(1')	(0.77576, 0.0584, 0.60887)	
Cd(1)	(0.72424, 0.5584, 0.10887)	
Cd(1)	(0.22424, 0.9416, 0.10887)	
C(7)	(0.3573, 0.67798, 0.3355)	(0.5, 0.5, 0.4281)
C(7)	(0.6427, 0.32202, 0.8355)	
C(7)	(0.8573, 0.82202, 0.3355)	

C(7)	(0.1427, 0.17798, 0.8355)
C(20)	(0.61078, 0.33337, 0.5207)
C(20)	(0.88922, 0.83337, 0.0207)
C(20)	(0.11078, 0.16663, 0.5207)
C(20)	(0.38922, 0.66663, 0.0207)

$(0.4281 - 0.35887) \times c \times Z \times e = 0.06923 \times 16.1558 \times 10^{-10} \text{ m} \times 4 \times 1.6 \times 10^{-19} \text{ C}$
$= 7.158 \times 10^{-29} \text{ C·m} = 21.459 \text{ D}$

(1): $\mu_c = 20.4735/ (3031.7 \times 3.7^2) = 4.93 \times 10^{-4} \text{ D/(Å}^3 \text{ eV}^2)$

(2): $\mu_c = 21.459/ (3075.6 \times 3.84^2) = 4.73 \times 10^{-4} \text{ D/(Å}^3 \text{ eV}^2)$

Table S10. Bond valence sum of Cd^{2+} and Zn^{2+} ions in **1** and **2**.

Compound	Bond	Bond distance (Å)	Bond valence	Sum
1	Zn–Br(1)	2.4729	0.417707867	1.962114995
	Zn–Br(2)	2.4217	0.479440665	
	Zn–Br(3)	2.3995	0.510189541	
	Zn–Br(4)	2.3680	0.554776922	
2	Cd–Br(1)	2.6549	0.438531197	2.107367332
	Cd–Br(2)	2.5926	0.51853033	
	Cd–Br(3)	2.5710	0.550296917	
	Cd–Br(4)	2.5388	0.600008888	

Table S11. Measured LIDTs of **1**, **2** and AGS for their crystals.

Compound	Damage energy (mJ)	Spot area (cm²)	LIDT (MW/cm²)	LIDT (× AGS)	LIDT (× KDP)
AGS	1.81	0.022698	7.97	1	
1	51.3	0.022698	226.01	28.36	0.87
2	45.2	0.022698	199.14	24.98	0.76

Table S12. The calculated frequency-dependent SHG coefficients of **1** and **2**.

Compound	Nonvanishing independent SHG coefficients	Largest SHG coefficient at 1064 nm (pm/v)
	d_{15}	0.34
1	d_{24}	0.26
	d_{33}	0.14
	d_{15}	0.32
2	d_{24}	0.24
	d_{33}	0.13

Figure S1. (a) The structure of **2** along the *c*-axis; (b) The inorganic and organic parts rotating along the *c* axis with 2_1 helical symmetry; (c) The organic layers in the *ac* plane; (d) The inorganic layers in the *bc* plane and their dipole moments. Hydrogen atoms are omitted for clarity.
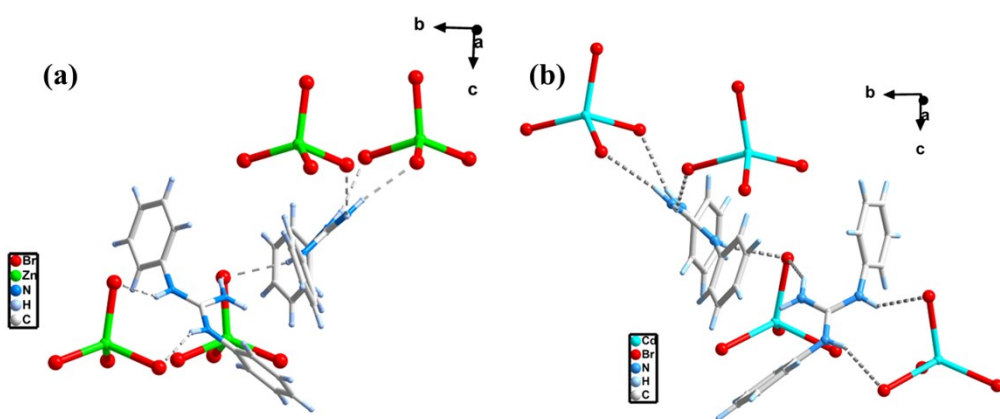
Figure S2. The hydrogen bonds in **1** (a) and **2** (b).
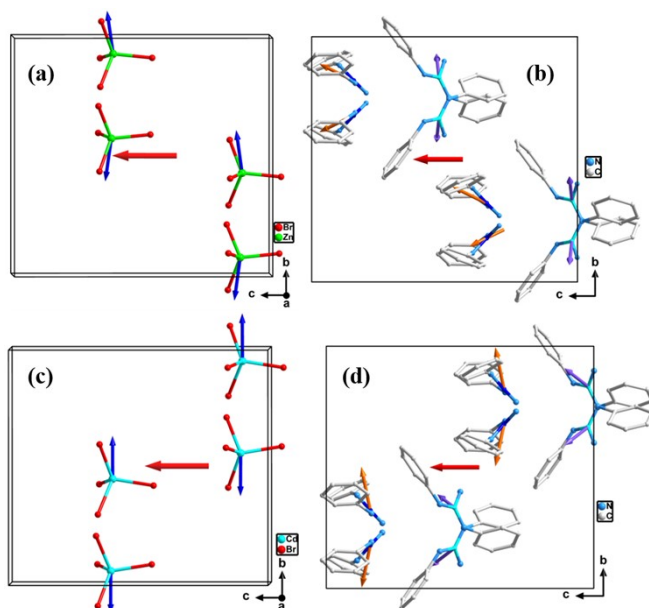
Figure S3. Dipole moments of $[MBr_4]^{2-}$ and $C_{13}N_3H_{14}^+$ ions in one-unit cell. (a) **1**; (b) **2**; Blue: $[MBr_4]^{2-}$; Orange and purple: $C_{13}N_3H_{14}^+$. The red arrows in the middle present the total dipole moments of the inorganic parts and organic parts, respectively.
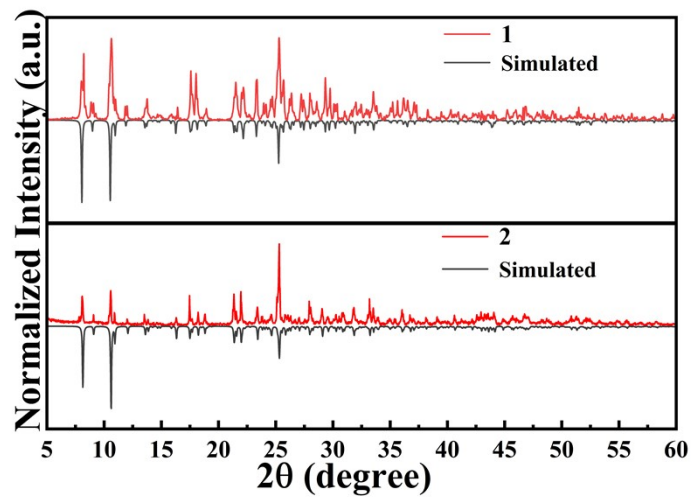
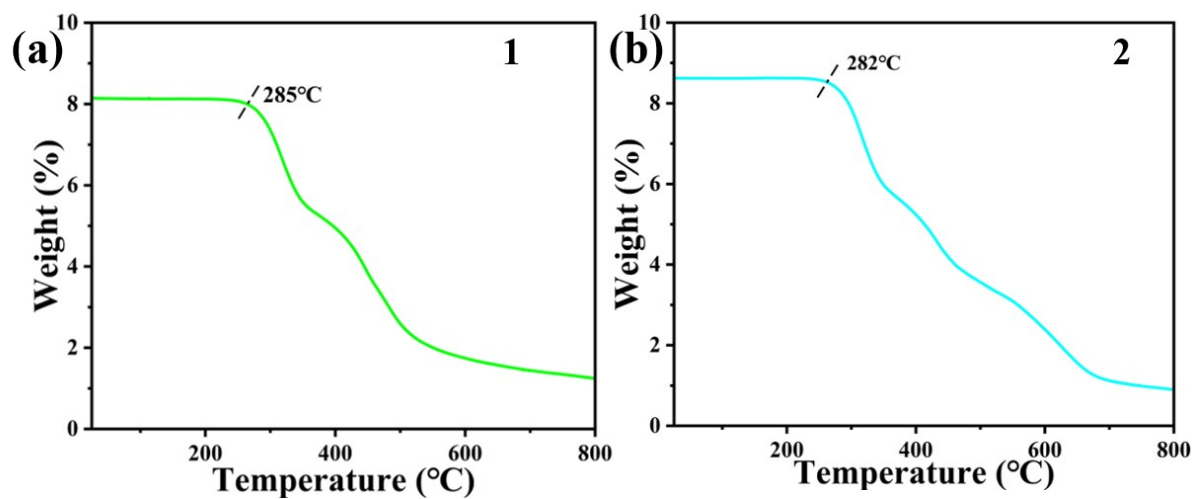**Figure S4.** Simulated and experimental powder X-ray diffraction patterns of **1** and **2**.

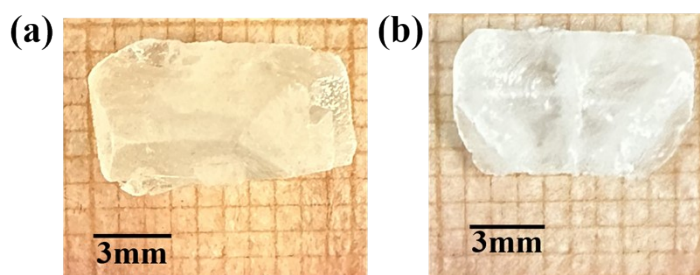**Figure S5**. The TGA curves of **1** (a) and **2** (b).

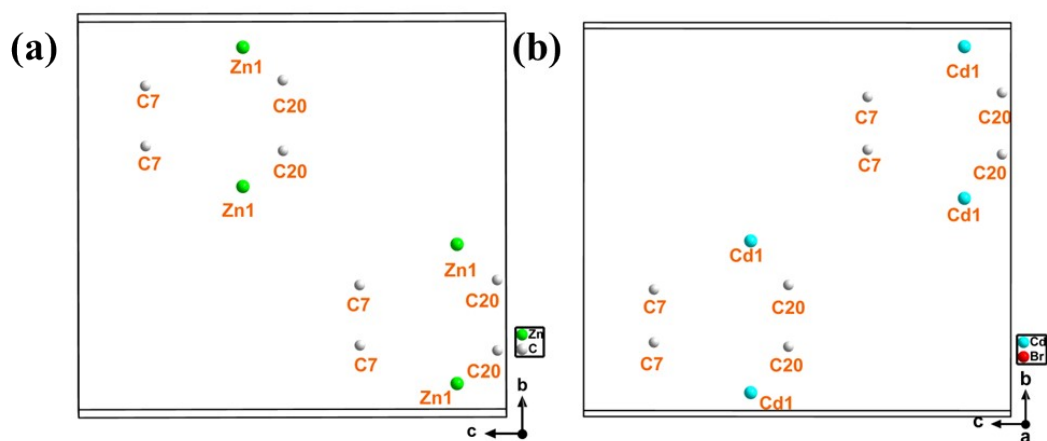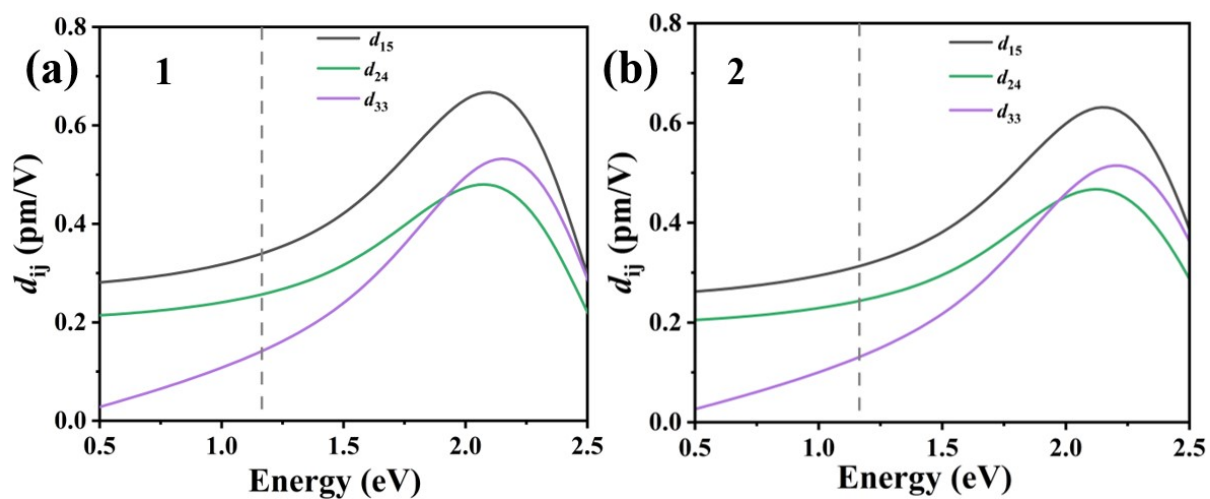**Figure S6.** Optical photographs of **1** (a) and **2** (b).

Figure S7. Distribution of C and Zn; C and Cd atoms in unit cells of **1** (a) and **2** (b).

Figure S8. Calculated frequency-dependent SHG coefficients of **1** (a) and **2** (b).

References

[1]. C. Yang, X. Liu, C. Teng, Q. Wu, F. Liang, Acentric Organic-Inorganic Hybrid Halide [N(CH$_3$)$_4$]$_2$HgBr$_2$I$_2$ Featuring an Isolated [HgBr$_2$I$_2$]$^{2-}$ Tetrahedron and Second-Order Nonlinearity, *Inorg. Chem.*, 2021, **60**, 6829–6835.

[2]. S. Wang, Z. Liang, X. Song, X. Huang, L. Liu, X. Jiang, Z. Lin, H. Liu, Photoluminescence and Nonlinear Optical Properties of Two Terpyridine-Based Hybrid Zn/Cd Halides, *Inorg. Chem.*, 2023, **62,** 21451–21460.

[3] J. L. Qi, J. J. Wu, Y. Guo, Z. P. Xu, W. L. Liu and S. P. Guo, Quasi-Linear CuX$_2$ (X = Cl, Br) Motif-Built Hybrid Copper Halides Realizing Encouraging Nonlinear Optical Activities, *Inorg. Chem. Front.*, 2023, **10**, 3319–3325.

[4]. Q. Wua, C. Yang, X. Liu, J. Ma, F. Liang, Y. S. Du, Dimensionality Reduction Made High-Performance Mid-Infrared Nonlinear Halide Crystal, *Mater. Today Phys.*, 2021, **21**, 100569.

[5]. L. He, Y. T. Liu, P. P. Shi, H. L. Cai, D. W Fu, Q. Ye, Energy Harvesting and Pd(II) Sorption Based on Organic-Inorganic Hybrid Perovskites, *ACS Appl. Mater. Interfaces.*, 2020, **12**, 53799–53806.

[6]. W. Q. Liao, H. Y. Ye, D. W. Fu, P. F. Li, L. Z. Chen, Y. Zhang, Temperature-Triggered Reversible Dielectric and Nonlinear Optical Switch Based on the One-Dimensional Organic−Inorganic Hybrid Phase Transition Compound [C$_6$H$_{11}$NH$_3$]$_2$CdCl$_4$, *Inorg. Chem.*, 2014, **53**, 11146−11151.

[7]. Z. Y. Bai, J. Y. Lee, H. Kim, C. L. Hu, K. M. Ok, Unveiling the Superior Optical Properties of Novel Melamine-Based Nonlinear Optical Material with Strong Second-Harmonic Generation and Giant Optical Anisotropy, *Small*, 2023, **19**, 2301756.

[8]. H. Y. Wu, C. L. Hu, M. B. Xu, Q. Q. Chen, N. Ma, X. Y. Huang, K. Z. Du, J. Chen, From H$_{12}$C$_4$N$_2$CdI$_4$ to H$_{11}$C$_4$N$_2$CdI$_3$: a Highly Polarizable CdNI$_3$ Tetrahedron Induced a Sharp Enhancement of Second Harmonic Generation Response and Birefringence, *Chem. Sci.*,2023, **14**, 9533–9542.

[9]. J. J. Wu, Y. Guo, J. L. Qi, W. D. Yao, S. X. Yu, W. L. Liu and S. P. Guo, Multi-Stimuli Responsive Luminescence and Domino Phase Transitionof Hybrid Copper Halides with Nonlinear Optical Switching Behavior, *Angew. Chem. Int. Ed.*, 2023, **62**, e202301937

[10]. L. H. Liu, Z. Y. Bai, L. Hu, D. S. Wei, Z. B, Lin, L. Z. Zhang, A Melamine-Based Organic-Inorganic Hybrid Material Revealing Excellent Optical Performance and Moderate Thermal Stability, *J. Mater. Chem. C.*, 2021, **9**, 7452–7457

[11]. X. Q. Ji, S. N. Geng, S. Zhang, Y. P. Gong, X. Y. Zhang, R. Q. Li, Y. Liu, J. Chen, R. Chen, Z. W Xiao, L. L. Mao, Chiral 2D Cu(I) Halide Frameworks, *Chem. Mater.*, 2022, **34**, 8262−8270.

[12] M. H. Choi, S. H. Kim, H. Y. Chang, P. S. Halasyamani, K. M. Ok, New Noncentrosymmetric Material-[N(CH$_3$)$_4$]ZnCl$_3$: Polar Chains of Aligned ZnCl$_4$ Tetrahedra. *Inorg. Chem.*, 2009, **48**, 8376−8382.

[13]. M. M. Zhao, L, Zhou, P. P. Shi, X. Zheng, X. G. Chen, J. X. Gao, F. J. Geng, Q. Ye, and D. W. Fu, Halogen Substitution Effects on Optical and Electrical Properties in 3D Molecular Perovskites, *Chem. Commun.*, 2018, **54**, 13275—13278.

[14]. C. Yang, X. Liu, C. L Teng, Q. Wu, F. Liang, Syntheses, Structure and Properties of a New series of Organic–Inorganic Hg-Based Halides: Adjusting Halogens Resulted in Huge Performance Mutations, *Dalton Trans.*, 2021, **50**, 7563–7570.

[15]. L. S. Li, Y. H. Tan, W. J. Wei, H. Q. Gao, Y. Z. Tang, X. B. Han, Chiral Switchable Low-Dimensional Perovskite Ferroelectrics, *ACS Appl. Mater. Interfaces.*, 2021, **13**, 2044−2051.

[16]. L. Zhou, X. Zheng, P. P. Shi, Z. Zafar, H. Y. Ye, D. W. Fu and Q. Ye, Switchable Nonlinear Optical and Tunable Luminescent Properties Triggered by Multiple Phase Transitions in a Perovskite-Like Compound, Inorg. Chem., 2017, 56, 3238–324416.

[17]. J. Cheng, Y. Deng, X. Dong, J. Li, L. Huang, H. Zeng, G. Zou andZ. Lin, Homochiral Hybrid Organic-Inorganic Cadmium Chlorides Directed by Enantiopure Amino Acids, *Inorg. Chem.*, 2022, **61**, 11032–11035.

[18]. C. Shen, J. Liu, K. Wu, L. Xu, D. Sun, Y. Dang, J. Wang and D. Wang, High stability and moderate second-order nonlinear optical properties of hybrid lead-free perovskite $[(CH_3)_3NCH_2Cl]CdCl_3$ bulk crystals, *CrystEngComm*, 2023, **25**, 2264–2270.

[19]. O. V. Dolomanov, L. J. Bourhis, R. J. Gildea, J. A. K. Howard, H. Puschmann, H. OLEX2: a complete structure solution, refinement and analysis program, *J. Appl. Crystallogr.*, 2009, **42**, 339−341.

[20]. Y. Guo, S. F. Yan, W. D. Yao, H. Y. Chen, W. l. Liu, J. J. Wu and S. P. Guo, Dual Monomeric Inorganic Units Constructed Bright Emissive ZeroDimensional Antimony Chlorides with Solvent-Induced Reversible Structural Transition, *Inorg. Chem.*, 2023, **62**, 13692-13697.

[21]. S. K. Kurtz, T. T. Perry, A powder technique for the evaluation of nonlinear optical materials, *J. Appl. Phys.*, 1968, **39**, 3798−3813.

[22]. M. D. Segall, P. L. D. Lindan, M. J. Probert, C. J. Pickard, P. J. Hasnip, S. J. Clark, M. C. Payne, First-principles simulation: ideas, illustrations and the CASTEP code, *J. Phys.: Condens. Matter.*, 2002, **14**, 2717−2744.

[23]. J. P. Perdew, K. Burke, M. Ernzerhof, Generalized gradient approximation made simple, *Phys. Rev. Lett.*, 1996, **77**, 3865−38685.

[24]. S. F. Li, X. M. Jiang, B. W. Liu, D. Yan, C. S. Lin, H. Y. Zeng, G. C. Guo, Superpolyhedron-Built Second Harmonic Generation Materials Exhibit Large Mid-Infrared Conversion Efficiencies and High Laser-Induced Damage Thresholds, *Chem. Mater.*, 2017, **29**, 1796–1804.

[25]. X. M. Jiang, G. E. Wang, Z. F. Liu, M. J. Zhang, G. C. Guo, Large Mid-IR Second-Order Nonlinear-Optical Effects Designed by the Supramolecular Assembly of Different Bond Types without IR Absorption, *Inorg. Chem.*, 2013, **52**, 8865–8871.